Article

Surface Modification and Spectroscopic Characterization of TiO$_2$ Nanoparticles with 2-Aminoethyl Dihydrogen Phosphate

Effat Iravani,[*,a] Sareh A. Allahyari,[a] Zahra Shojaei[b] and Meisam Torab-Mostaedi[a]*

[a] *Nuclear Science & Technology Research Institute, P.O. Box 11365-8486 Tehran, Iran*

[b] *Department of Chemical Engineering, Faculty of Engineering, Tehran University,
P.O. Box 11365-4563 Tehran, Iran*

A common strategy for the surface modification of nano TiO$_2$ and other metal oxide nanoparticles is based on anchor groups using chelating ligands that can carry additional functionalities. This would allow the exploration of further applications of these materials. In the present work, we report the modification of TiO$_2$ nanoparticles from nano TiO$_2$ (Degussa P-25) dispersion in distilled water in the presence of 2-aminoethyl dihydrogen phosphate, followed by removing the excess of the capping agent through washing with water. The surface functionalization and the kind of surface interaction were analyzed applying different characterization methods like CHN elemental analysis, thermogravimetric analysis (TGA), Fourier transform infrared spectroscopy (FTIR), attenuated total reflectance (ATR-FTIR), X-ray powder diffraction (XRD) and ^{1}H, ^{13}C, ^{31}P magic angle spinning nuclear magnetic resonance spectroscopy (MAS NMR), confirming the presence of modifying agent on the surface. In the study of modified nano TiO$_2$ by MAS NMR spectroscopy, a distinct downfield shift for ^{31}P signal has been seen comparing to the pure cappping agent due to P–O–Ti bond formation. The phosphate groups interact with the surface via quite strong covalent interaction, while according the analyses results, the surface amine groups remained uncoordinated.

Keywords: nano TiO$_2$, surface modification, solid state ^{31}P MAS NMR

Introduction

Among the various nanoparticles, nano TiO$_2$ possesses industrial applications as pigments, dye-sensitized solar cells,[1] filters for catalyst supports, and photocatalysis,[2] because of interesting optical, dielectric and catalytic properties. Hydroxyapatite-titania composites provide biocompatible materials.[3] Moreover being nontoxic, TiO$_2$ promises to create chemical and biological hybrid nanocomposites that can be introduced into cells and can further be used to initiate intracellular processes as well as biotracers.[4]

In the design of compatible nanoparticles, the selection of the nanostructured core and its surface modification with polymers, organic or inorganic materials plays the major role affecting the performance of nanoparticles in the biomedical applications. Surface modification is important for ensuring the biocompatibility. López *et al.*[5] used sulfate, amine and phosphate ions separately as functional groups, which were anchored to the titania's surface to obtain a biocompatible material to be used as carrier of alternative anticancer agents. Niederberger *et al.*[6] described the synthesis of anatase TiO$_2$ nanoparticles with an amine functionalized surface.

We were interested in surface modifying of nano TiO$_2$ (due to being nontoxic) to obtain a kind of anchor group for immobilization of biomolecules in the future. The possible capping agents include alcohols, carboxylic acids, silanes, sulfonic acids, phosphoric acids and phosphonic acids.[7] Different derivatives of phosphonic acids were first used as capping agent on metal oxide surfaces in the early nineties.[8] Phosphates have also been used to anchor some multifunctional organic molecules on TiO$_2$ surface as self-assembled monolayers.[9] It is known from literatures that phosphoric acid, phosphonic acid, phosphinic acid and some of their derivatives usually interact with metal oxide surfaces by formation of strong chemical bonds.[10, 11]

In order to benefit the advantageous of having two functional groups namely amine and phosphate on a unique molecule as coupling agent, 2-aminoethyl dihydrogen phosphate (AP) seemed to be a suitable candidate to modify nano TiO$_2$ surface. Also the surface of nano

*e-mail: iravanieffat@yahoo.de

TiO$_2$ (Degussa P-25) was modified with AP. Modified nano TiO$_2$ was characterized through Fourier transform infrared spectroscopy (FTIR), attenuated total reflectance Fourier transform infrared (ATR-FTIR) and solid state magic angle spinning nuclear magnetic resonance (MAS NMR) spectroscopy. Other analytical methods like scanning electron microscope (SEM), transmission electron microscopy (TEM), elemental analysis (CHN), thermogravimetric analysis (TGA) and X-ray powder diffraction (XRD) were used to complete the identification of amino functionalized nano TiO$_2$ (AP-nano TiO$_2$).

Experimental

Materials

Nano TiO$_2$ with a purity of 99.5% (21 nm average particle size) was purchased from Degussa, Germany and used as obtained for surface modification. AP was purchased from Merck, Germany with a purity of 98% and purified through recrystallization from distilled water before using. D$_2$O (99.9 atom%) and orthophosphoric acid (85%) were aquired from Aldrich, Germany. Ethanol (99.5%) obtained from Bidestan, Iran and distilled water were used for the reaction and washing proccess. The chemicals used in the ninhydrin dye test were ethyl acetate (99.9%, Fluka, Germany), ninhydrin ($\geq$ 99%, Merck), acetic acid (100%, Merck) and heptane (99%, Aldrich).

Methods

FTIR spectra were recorded with KBr pellets on a Bruker Vector 22 FTIR spectrometer. Attenuated total reflectance spectra were recorded on a Bruker Tensor 27 ATR-FTIR spectrometer equipped with a ZnSe single crystal. ^{1}H, ^{13}C and ^{31}P NMR spectra in liquid phase were recorded on a Bruker Topspin spectrometer 500 MHz in D$_2$O as the solvent. Chemical shifts (δ) were reported relative to internal standard Me$_4$Si (TMS, δ = 0.00 ppm). Orthophosphoric acid (85%) was used as the external standard (δ = 0.00 ppm) for ^{31}P NMR measurement in liquid phase. NMR spectra including ^{1}H, ^{31}P MAS NMR and ^{13}C CP/MAS NMR spectra were recorded on Bruker Avance Spectrospin 400 MHz and Bruker Topspin spectrometer 500 MHz respectively. The XRD patterns were recorded with a Stoe Stadi-Mp diffractometer (40 kV, 30 mA), equipped with a Cu K$_\alpha$ radiation source (λ = 1.5418 Å). TGA analyses were performed on a Rheometricscientific Sta 1500 thermal analyser under air flow with the heating rate of 10 °C min^{-1} and temperature range 25-900 °C. Specific surface area measurement was

done with Covanto Crom-Nova 2000 apparatus. The adsorption gas was nitrogen. High resolution transmission electron microscope (HRTEM) image and scanning electron microscope image were obtained with a Jeol 3010 microscope at 300 kV and REM CamScan-4DV respectively.

Modification of nano TiO$_2$ with AP

AP (0.141 g, 0.001 mol) was dissolved in 100 mL distilled water. Nano TiO$_2$ (0.799 g, 0.01 mol) was added into the AP solution and stirred for 24 h at room temperature. Then the mixture was centrifuged for 30 min with a ramp of 6000 cycle min^{-1}. The resulted powders were eluted with distilled water and afterward dried in an oven at 100 ºC for 12 h.

Preparation of ninhydrin solution

2,2-Dihydroxyindane-1,3-dione (0.2 g, 0.001 mol) was dissolveld in a solution of ethyl acetate (1 mL), ethanol (3 mL), heptane (0.04 mL) and acetic acid (0.12 mL).[11] It was also possible to prepare the solution without acetic acid. The difference would be observed in different colors. Ninhydrin solution with acetic acid leads to hell violet color, while the absence of acetic acid in ninhydrin solution results in dark violet color, if the test is positive.

Results and Discussion

SEM and HRTEM analyses

Figure 1 shows the HRTEM and SEM images of AP functionalized TiO$_2$ nanoparticles. The micrographs showed that the nano TiO$_2$ particles after modification (treatment with AP) were well dispersed and had fairly homogeneous and spherical shape. According to the HRTEM and SEM micrographs of the treated nano TiO$_2$ it could be clearly seen in Figure 1 that non considerable agglomeration happened during treatment of nano TiO$_2$ with AP.

CHN, BET analyses and surface coverage of AP-nano TiO$_2$

Surface coverage percentage and number of AP molecules *per* square nanomer of nano TiO$_2$ were calculated from the CHN elemental analysis results and the surface area of the AP-nano TiO$_2$ obtained by nitrogen sorption measurements (BET).

Using CHN elemental analysis, the AP content of modified nano TiO$_2$ was calculated. As shown in Table 1,
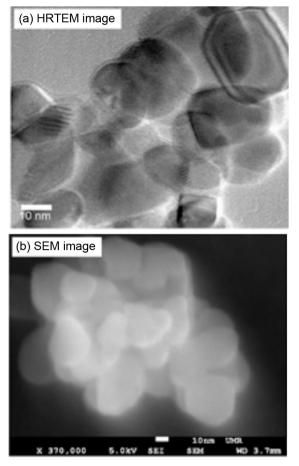
Figure 1. (a) HRTEM and (b) SEM images of AP-nano TiO$_2$.

the measured H/C ratio for AP-nano TiO$_2$ is a little more than the calculated one for pure AP, that could be due to the free hydroxyl groups on nano TiO$_2$ surface, which are not bonded to AP.

Table 1. Elemental analysis of AP-nano TiO$_2$

	AP (Theoretical value)	AP-nano TiO$_2$ (Experimental value)
C / wt.%	16.95	0.539
H / wt.%	5.65	0.253
N / wt.%	9.89	0.306
H/C	0.33	0.47

According to BET analysis result, the surface area of AP-nano TiO$_2$ (55.78 m^2 g^{-1}) is slightly higher than untreated nano TiO$_2$ (about 50 m^2 g^{-1}). By means of BET surface area of AP-nano TiO$_2$ and its mass percentage obtained from the carbon values of CHN analysis (0.539 wt.%) (Table 1), the amount of amino phosphate groups on the surface of modified nano TiO$_2$ was calculated to be about 3.17 wt.% and the number of coupling agent (AP) conjugated to the surface was estimated ca. 2.43 molecules AP *per* nm^2.

The calculated surface density was higher than the value reported for functionalized bulk TiO$_2$ powder,[12] which seemed to be logic due to the less surface area of bulk TiO$_2$ powder (about 9.45 m^2 g^{-1}) compared with nano TiO$_2$ (about 50 m^2 g^{-1}).

Short alkyl phosphates are mainly stabilized due to their interaction with the surface. This might be the reason that they do not pack as densely in order to bind at an optimal place in a strong bridging or chelating bidentate manner, which can be further stabilized by hydrogen bonds to free surface Ti–OH groups.[13]

TGA analysis

All samples were dried at 100 ℃ for two hours before TGA measurement. Pure AP began at about 274 ℃ to loose weight and decomposed to a gray substance. If this substance would be P$_4$O$_{10}$, according to the calculation it would be expected to reach a mass loss about 50 wt.%, but it was just about 90.11 wt.% at the end of heating at 900 ℃, which was understandable due to the sublimation of P$_4$O$_{10}$ around 360 ℃. The remained mass stayed by about 10 wt.%. Fire retardancy of organophosphorus compounds could be the reason of unburnable residue. TGA curve of AP-nano TiO$_2$ remained straight till about 600 ℃ without any weight loss and after that began to lose weight. Decomposition temperature for AP-capped nano TiO$_2$ particles was high (about 600 ℃). This fact could be a proof, that there is not much free capping agent in AP-modified nano TiO$_2$ (Figure 2). AP content of AP-nano TiO$_2$ according to TGA analysis under air flow, was slighlty higher compare to the calculated amount from elemental analysis results: 3.73 wt.% and 3.17 wt.% respectively.
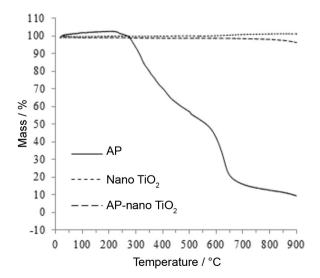

Figure 2. TGA of AP, nano TiO$_2$, and AP-nano TiO$_2$ under air flow.

FTIR spectroscopy

In general primary amines can be identified by two sharp absorption bands around 3500-3300 cm^{-1}, which are approximately 70 cm^{-1} apart, caused by v_s(-NH$_2$) and v_{as}(-NH$_2$). FTIR spectrum of AP-nano TiO$_2$ (Figure S1) showed a broad strong band in the upper side centered at 3411 cm^{-1} originated by the stretching vibration of O–H (water molecules and the free remained surface hydroxyl groups of nano TiO$_2$). Superimposed were the NH stretching vibrations of the amine. O=P–(OH)$_n$ (n = 1, 2) IR bands involving O–H stretching vibration appear generally in the range of 2725-1600 cm^{-1} with maxima at 2350-2080 cm^{-1}, and 1740-1600 cm^{-1}.[14] The last peak at 1740-1600 cm^{-1} is the strongest for n = 1 and the weakest, if present at all for n = 2.[14] The first peak assigned to O=P–(OH)$_2$ for AP around 2125 cm^{-1} was not clearly to see for modified nano TiO$_2$ because of broadening, and the second one centered at 1629 cm^{-1} was the strongest, which seemed to be overlapped with the bending mode of water molecules (OH) and amine groups (NH) too. Due to broadening and overlapping of the related peaks, it was not easy to judge about the existence of P–OH. The existence of P=O bond can be proved generally by an absorption band in the range of 1320-1140 cm^{-1} related to stretching vibration mode, which was observed at 1269 cm^{-1} as a weak peak. The pattern of the spectrum for AP-nano TiO$_2$ in the range of 1270-1074 cm^{-1} contained some bands similar to this pattern in the FTIR spectrum of AP. These features together with TGA and CHN elemental analyses thereby verified the existance of AP on the surface of nano TiO$_2$ particles after modification procedure. The peaks related to organophosphorus coupling agent were not strong due to relatively low degree of functionalization. Predicting the AP bonding mode onto the surface of nano TiO$_2$ only with FTIR spectrum was not possible.

ATR-FTIR spectroscopy

ATR-FTIR spectroscopy is a technique capable of characterization of the nanoparticle surfaces. In this method of sample preparation, a beam of light incidents a crystal of high refractive index (n$_c$) at θ (the angle of incidence), which encounters a boundary with a sample with lower refractive index (n$_s$). The generated standing evanescent wave penetrates into the surface and interacts with the sample. The depth of penetration (DP) given by equation 1 is the depth at which the evanescent wave intensity decreases to 36.8% of its initial value. DP is rarely greater than 10 μm and can be less than 1 μm (W is the wavenumber).

$$DP = 1 \Big/ \left[2 \quad {}_c \left({}^2 \quad {}^2_s \Big/ {}^2_c \right)^{1/2} \right] \tag{1}$$

The shallow spectral sampling depth also provides a unique opportunity and ideal technique for investigating the chemical interactions occurring at particulate surfaces. It is noteworthy to mention that in general ATR can detect molecules present in concentrations greater than 0.1%.[15] According our calculaton after CHN and BET results, there was about 3.17 wt.% AP in AP-nano TiO$_2$. ATR-FTIR spectrum of AP-nano TiO$_2$ was obtained to investigate the existence of AP molecules on the surface of nano TiO$_2$ after modifying more precisely.

On the other hand the dependence of ATR intensities on wavenumber has important implications for how we can use and interpret ATR spectra. It is difficult to compare ATR spectra to spectra measured using other sampling techniques because the spectra of the same sample will look different. This is why it is best to only compare ATR spectra to other ATR spectra. If one must compare ATR and non-ATR spectra to each other, should be aware that the relative intensities will be different. That was the reason to obtain the ATR spectra of AP and nano TiO$_2$ besides AP-nano TiO$_2$ to be able to compare all the spectra.[15]

Around 3000 cm^{-1} there were two sharp bands centered at 2933 and 2901 cm^{-1} related to symmetric and asymmetric stretching vibration of –CH$_2$– groups of AP, which demonstrated the presence of organic material into nano TiO$_2$ matrix (Figure S2). Due to high penetration depth of light in FTIR technique, the light penetrates into not only the surface, but the bulk sample. Because of low surface coverage with AP, the absorption bands of coordinated AP onto nano TiO$_2$ surface in FTIR spectrum were very weak in comparison with ATR-FTIR absorption bands. The mentioned bands were not obviously seen in the FTIR spectra. There were similarity between the ATR spectrum of pure AP and the one of the AP-nano TiO$_2$, suggesting that AP functionalization of nano TiO$_2$ was done successfully. This was not possible to detect NH$_2$ groups via ATR spectrum of AP-nano TiO$_2$, which could be probably a hint of existence of AP in the form of zwitterion.[12]

Ninhydrin test

Due to the broad band centered at 3411 cm^{-1} related to hydroxyl groups and water molecules on the surface of modified nano TiO$_2$, it was not easy to discuss about amine stretching vibration bands. Because of this fact, ninhydrin test was chemically used to investigate the presence of free amine groups in AP-nano TiO$_2$. Untreated nano TiO$_2$ (as the reference) and AP-nano TiO$_2$ were separately soaked in ninhydrin solution. After drying, the color of modified

sample (AP-nano TiO$_2$) changed from white to hell violet, which confirmed the presence of amines; there was no color change to observe for the untreated nano TiO$_2$ (Figure S3).

Powder XRD measurement

Typical XRD patterns obtained for the pure nano TiO$_2$ (a), AP (b), AP-nano TiO$_2$ (c) and AP-nano TiO$_2$ after thermal treatment (d) were shown in Figure 3. The diffraction pattern of pure nano TiO$_2$ coincided well with that of nano TiO$_2$ (P-25). Except for nano TiO$_2$ peaks, the other observed peaks in the 2θ range of about 15-28 degrees for AP-nano TiO$_2$ could be probably resulted from the remained AP as impurity on the spatula or agate mortar during sample preparation processes for nano-TiO$_2$, Ap and AP-nano TiO$_2$. We suggest that hydrolyzed or dissolution-precipitation products should be washed away. However the mentioned byproducts as a possible source of the impurity peaks could not be ruled out. The modifier showed no obvious effect on the structure of nano TiO$_2$.

The XRD pattern of AP-nano TiO$_2$ after thermal treatment at 700 °C matched well nano TiO$_2$ and the standard diffraction lines of titanium pyrophosphate with the reference code 00-038-1468. This was a proof for the stability of Ti–O–P bond.

^{1}H MAS NMR spectroscopy

The results of NMR spectroscopy often provide information which is sometimes unattainable by other spectroscopic techniques. The development of NMR spectrometers with high magnetic fields and the line narrowing techniques made it possible to obtain high resolution NMR spectra of solid surfaces and adsorbed species at very low coverage.

^{1}H MAS NMR spectrum of nano TiO$_2$ P25 measured at the spinning rate of 12.6 kHz presents a single signal.[16] According to the temperature dependent ^{1}H MAS NMR studies, anatase nano TiO$_2$ samples possess the positively charged acidic protons located on bridged O atoms (δ 6.4 ppm), and the basic H atoms bound to the terminal oxygen (δ 2.3 ppm).[17]

^{1}H MAS NMR spectrum of AP-nano TiO$_2$ in powder form measured at room temperature (Figure 4) presented a single broad signal with a chemical shift of 9.64 ppm, which was ascribed to the relatively mobile physisorbed water and surface hydroxyl groups not bonded to AP. The low-field chemical shift of the ^{1}H signal for AP-nano TiO$_2$ comparing with the reported one for nano TiO$_2$ by Nosaka *et al.*[16] might indicate the existence of more abundant acidic H atoms from N$\underline{H}_2$ or probably PO$\underline{H}$ along with surface hydroxyl groups. The ^{1}H resonance line was
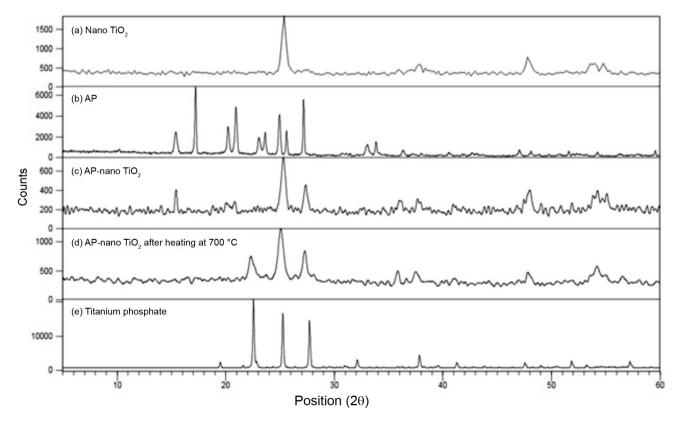

Figure 3. XRD patterns of (a) nano TiO$_2$; (b) AP; (c) AP-nano TiO$_2$ before and (d) after heating at 700 °C and (e) titanium phosphate.

intense and broad with a line width of more than 1 kHz at half peak height. Methylene (N−C$\underline{H}_2$, O−C$\underline{H}_2$), amine (N$\underline{H}_2$) and P−O$\underline{H}$ signals of AP were not observed probably due to overlapping with the adsorbed water molecules and surface hydroxyls signal of nano TiO$_2$.
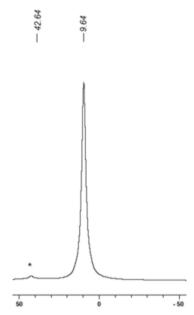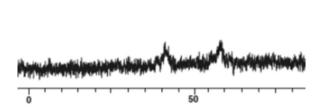

Figure 4. ^{1}H MAS NMR spectrum of AP-nano TiO$_2$, peak marked with * indicates the spinning band.

^{13}C CP/MAS NMR spectroscopy

For most of organophosphorus compounds, the acid catalyzed hydrolysis is fairly slow and is thus negligible under environmental reaction conditions, whereas neutral and alkaline hydrolysis are of concern.[18] The hydrolysis reaction rate is indeed a function of both the nucleophile and the leaving group acidity.[19] In our study the reaction mixture of AP and nano TiO$_2$ was acidic (pH = 3.15) and the hydrolysis of AP under acidic pH seemed not to be easy, anyway we liked to investigate, if chemisorbed AP molecules undergo hydrolysis route. To investigate this point, Cross polarization magic angle spinning solid state ^{13}C NMR spectroscopy was used as a valuable tool. Individual AP molecules exhibit two resonances at ca. 40.17 ppm and 61.43 ppm in the solution ^{13}C NMR spectrum while, after its reaction with nano TiO$_2$, these resonances moved to the weaker and stronger field regions (41.48 ppm, 58.12 ppm) of the spectrum, respectively (Figure 5). This confirmed that aminoethyl chain stayed on the phosphate groups and AP was not hydrolyzed.

Upfield shift of O−$\underline{C}$ signal about 3.31 ppm comparing with coupling agent (AP, δ_{O-C} 61.43 ppm) was a proof cue AP bonding with nano TiO$_2$ through phosphate groups. Such shielding effect was reported for modified bulk TiO$_2$.[12]

Figure 5. ^{13}C CP/MAS NMR spectrum of AP-nano TiO$_2$.

As mentioned before, surface coverage (2.43 molecules AP *per* nm^2) was not very high and could probably make it possible for aminoethyl chain lying parallel to the surface and forming hydrogen bonds with the surface hydroxyl groups consequently. This hypothesis regarding amino groups positions on the treated nano TiO$_2$ agreed with the ^{13}C CP/MAS NMR spectral result, and caused a downfield shift ca. 1.31 ppm in the ^{13}C CP/MAS NMR signal of N−$\underline{C}$.

^{31}P MAS NMR spectroscopy

^{31}P MAS NMR spectrum of AP-nano TiO$_2$ exhibited a broad main signal, as expected for phosphorus in a large range of environment (Figure 6). Another reason for the broadening of ^{31}P signal for AP-nano TiO$_2$ could be dipole-dipole interaction between ^{31}P and probable existing ^{1}H nucleus. The ^{31}P MAS NMR signal of AP-nano TiO$_2$ showed a significant shift from 0.17 ppm for AP to 2.11 ppm due to the formation of Ti−O−P.
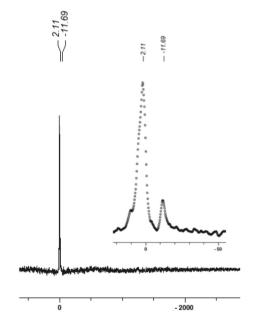

Figure 6. ^{31}P MAS NMR spectrum of AP-nano TiO$_2$.

The ^{31}P MAS NMR spectra of AP-nano TiO$_2$ with and without ^{1}H high-power decoupling were shown in Figure 7. The dipole-dipole interaction between ^{1}H and ^{31}P caused a broadening of the signal of ^{31}P in the MAS-only spectra (Figure 7b). The high-power decoupling technique diminishes this interaction by saturating the magnetization of ^{1}H nuclei and brings about a sharp resonance line, as can be seen in Figure 7a. In this way one can distinguish protonated and unprotonated phosphate groups. The broad peak at 2.11 ppm in the spectrum of AP-nano TiO$_2$ without ^{1}H decoupling indicated strong ^{1}H and ^{31}P dipole-dipole interactions. Therefore, the peak at 2.11 ppm could be assigned to a ^{31}P with OH group.

Figure 8. Reaction of AP with nano TiO$_2$: (a) surface modification; (b) competition between surface modification and dissolution-precipitation.

Dissolution of CaCO$_3$ and precipitation of calcium alkylphosphate salts has been reported in the surface modification of CaCO$_3$ powders by alkylphosphoric acids.[7]

^{31}P NMR data of various titanium phosphates have been reported. Studies of titanium phosphates of known crystal structures have shown a correlation between connectivity and chemical shift. As the connectivity for titanium phosphate increases, an upfield shift is observed from −5.3 to −10.6 ppm for H$_2$PO$_4^-$ unit to −18.1 ppm for HPO$_4^-$ unit.[20] A comparison of the positions of the signals obtained with the reported data indicated that the difference from 2.11 ppm (stark peak) to −11.69 (weak peak) might be attributed to a kind of titanium (organo) phosphate.

Bonding mode

AP can, in principle, bind to a transition metal oxide surface in either a monodentate, bidentate or even tridentate manner as illustrated in Figure 9. Additionally, the bonds can be either formed in a bridging or chelating fashion leading to a large variety of interaction between AP and the surface of nano TiO$_2$. The binding of ^{17}O−enriched phosphonic acids derivatives chemisorbed on titanium dioxide was studied by high-field NMR studies earlier.[21] The presence of P−O−Ti, P=O, and P−OH indicated that mono-, bi- and tridentate surface phosphonate units can be present in these monolayers. The chemical shift of the P−O−Ti sites was found to be consistent with bridging modes, negating the possibility of anchoring through chelating modes.[21]

In the single-crystal structures of layered alkyl phosphates, the phosphate groups bind almost in a bridged binding mode. Two and three-fold coordination can be
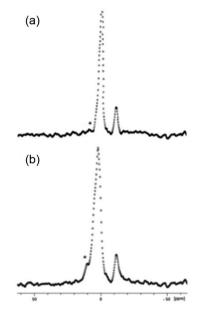

Figure 7. ^{31}P MAS NMR spectra of AP-nano TiO$_2$ (a) with and (b) without ^{1}H decoupling. Peak marked with * is due to impurity.

There was another signal with a chemical shift of −11.69 ppm. Two categories of compound**s** namely hydrolysis product and dissolution-precipitation product might be responsible for this signal. P−O−C bonds are quite stable toward hydrolysis, and homocondensation of P−O−H bonds with formation of P−O−P bonds takes place only under high temperature dehydrating conditions.[7] The result of ^{13}C CP/MAS NMR for AP-nano TiO$_2$ has confirmed, that alkyl chain stayed on AP after modification reaction.

It has been shown that in surface modification with organophosphorus coupling molecules, depending on the chemical stability of the transition metal oxide and the reaction conditions, a dissolution-precipitation process may compete with surface modification, leading to the formation of a metal phosphate phase (Figure 8), even in the case of chemically stable oxides such as TiO$_2$.[7]
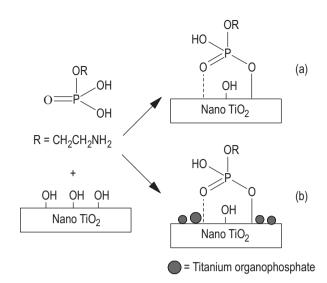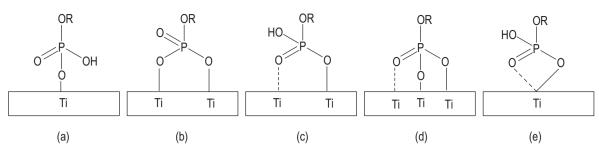
Figure 9. Schematic representation of binding modes between AP and nano TiO_2: (a) monodentate; (b) bidentate; (c) bridging bidentate; (d) bridging tridentate; (e) chelating bidentate (adapted from reference 21).

found, while a chelating binding mode with two oxygen atoms binding to the same metal is very uncommon.[13] We can most probably exclude such a chelating binding mode, since this would be lead to coordination numbers for the titanium of larger than six, and a highly strained four-numbered Ti–O–P–O cycle, which should not be energitically favorable. Connor *et al.*[22] have studied earlier the adsorption of phosphates (ionic and substituted) onto TiO_2 and showed that phosphate species bind to TiO_2 predominantly bidentate in neutral and acidic aqueous solution. Contribution of phosphate groups in bidentate bridging coordination of AP onto nano TiO_2 surface (Figure 9: (b) or (c)) is pH dependent. pK_{a1} of AP is less than phosphoric acid and more than dihydrogen phosphate (Table 2).

Table 2. pK_a for AP, acid and bases[10]

	pK_{a1}	pK_{a2}	pK_{a3}
AP	5.61	10.39	–
H_3PO_4	2.15	7.20	12.37
Primary amines	36	–	–
NH_3	9.25	–	–

The reaction mixture of AP and nano TiO_2 was acidic and showed a pH about 3.51. We may conclude, that it is not easy for AP to loose its second proton in such an acidic aqueous solution. Accordingly, the interaction of AP with nano TiO_2 surface in a form of bridging bidentate through P=O and P–OH is more favorable, however we can not neglect the mono- and tridentate binding mode.

Conclusions

Nano TiO_2 (P-25) with a diameter of around 21 nm was functionalized with AP in acidic pH conditions. Through different characterization methods including ATR-FTIR, solid state NMR spectroscopy and powder XRD studies it was confirmed that AP was chemisorbed onto the nano TiO_2 surface. In spite of good hydrolytic stability of P–O–C bonds, allowing the use of some organophosphates like AP

as coupling molecules, a dissolution-precipitation process, leading to the formation of metal phosphate phase, could occur depending on the chemical stability of the inorganic substrate and the reaction conditions. We found that such molecules with a short alkyl chain (AP) assembled into a less dense structure. This was supported by the fact that there was an excess of hydrogen found for AP-nano TiO_2, which we interpreted as free surface Ti–OH groups.

Supplementary Information

Supplementary Information is available free of charge at http://jbcs.sbq.org.br as PDF file.

Acknowledgements

References

1. Ramakrishna, G.; Ghosh, H. N.; *J. Phys. Chem. B* **2001**, *105*, 7000.

2. McFarland, E. W.; Tang, J.; *Nature* **2003**, *421*, 616.

3. Kim, H. W.; Kim, H. E.; Salih, V.; Knowles, J. C.; *J. Biomed. Mater. Res. B* **2005**, *72*, 1.

4. Paunesku, T.; Rajh, T.; Wiederrecht, G.; Maser, J.; Vogt, S.; Stojicevie, N.; Protic, M.; Lai, B.; Oryhon, J.; Thurnauer, M.; Woloschak, G.; *Nat. Mater.* **2003**, *2 (5)*, 343.

5. LóPez, T.; Ortiz, E.; Guevara, P.; Gómez, E.; Novaro, O.; *Mater. Chem. Phys.* **2014**, *146*, 37.

6. Niederberger, M.; Garnweitner, G.; Krumeieh, F.; Nesper, R.; Coelfen, H.; Antonietti, M.; *Chem. Mater.* **2004**, *16*, 1202.

7. Mutin, P. H.; Guerrero, G.; Vioux, A.; *J. Mater. Chem.* **2005,** *15*, 3761.

8. Guang, C.; Hong, H. G.; Mallouk, T. E.; *Acc. Chem. Res.* **1992,** *25*, 420.

9. Gnauck, M.; Jaehne, E.; Blaetter, T.; Tosatti, S.; Textor, M.; Adler, H. J.; *Langmuir* **2007**, *23 (2)*, 377.

10. Kakihana, M.; Nagumo, T.; Okamoto, M.; Kakihana, H.; *J. Phys. Chem.* **1987**, *91*, 6128.

11. Paunikallio, T.; Suvanto, M.; Pakkanen, T. T.; *J. Appl. Polym. Sci.* **2006**, *102*, 4478.

12. Myller, A. T.; Karhe, J. J.; Pakkanen, T. T.; *Appl. Surf. Sci.* **2010**, *257*, 1616.

13. Spori, D. M.; Venkataraman, N. V.; Tosatti, S. G.; Durmaz, F.; Spencer, N. D.; Zuercher, S.; *Langmuir* **2007**, *23(15)*, 8053.

14. E. Glaser, R,; Hampton, C.; Demoin, D; *Vibrational Spectroscopy Tutorial: Sulfur and Phosphorus*, available at http://faculty.missouri.edu/~glaserr/8160f10/A03_Silver.pdf accessed in May 2015; Yamaji, T.; Saito, T.; Hayamizu, K.; Yanagisawa, M.; Yamamoto, O.; Wasada, N.; Someno, K.; Kinugasa, S.; Tanabe, K.; Tamura, T.; *Spectral Database for Organic Compounds* (*SDBS*), National Institute of Advanced Industrial Science and Technology, http://sdbs.db.aist.go.jp/sdbs/cgi-bin/direct_frame_top.cgi accessed in April 2015.

15. Smith, B. C.; *Fundamentals of Fourier Transform Infrared Spectroscop*y; CRC Press: New York, USA, 2011.

16. Nosaka, A. Y.; Nosaka, Y.; *Bull. Chem. Soc. Jpn.* **2005**, *78*, 1595.

17. Mastikhin, V. M.; Mudrakovsky, I. L.; Nosov, A. V.; *Prog. Nucl. Magn. Reson. Spectrosc.* **1991**, *23*, 259.

18. Draber, W.; Fujita, T.; *Rational Approaches to Structures, Activity, and Ecotoxicology of Agrochemicals*, CRC Press: Florida, USA, 1992.

19. Wickman, J. R.; Halye, J. L.; Kashtanov, S.; Khandogin, J.; Rice, C. V.; *J. Phys. Chem. B* **2009**, *113*, 2177.

20. Jones, D. J.; Aptel, G.; Brandhorst, M.; Jacquin, M.; Jimenez-Jimenez, J.; Jimenez-Lopez, A.; Maireles-Torres, P.; Piwonski, I.; Rodriguez-Castellon, E.; Zajac, J.; Roziere, J.; *J. Mater. Chem.* **2000**, *10*, 1957.

21. Paz, Y.; *Beilstein J. Nanotechnol.* **2011**, *2*, 845.

22. Connor, P. A.; McQuilan, A. J.; *Langmuir* **1999**, *15 (8)*, 2916.